POLITECNICO DI TORINO
Repository ISTITUZIONALE

Empirical mode decomposition analysis of near-infrared spectroscopy muscular signals to assess the effect of physical activity in type 2 diabetic patients

(Article begins on next page)

16 April 2024

Empirical Mode Decomposition Analysis of Near-Infrared Spectroscopy Muscular Signals to Assess the Effect of Physical Activity in Type 2 Diabetic Patients

Filippo Molinari[1], Roshan Joy Martis[2], U Rajendra Acharya[3,4], Kristen M. Meiburger[1], Riccardo De Luca[5],

Giuliana Petraroli[5], William Liboni[6]

[1] Biolab, Department of Electronics and Telecommunications, Politecnico di Torino, Torino, Italy

[2]Department of Electronics and Communication Engineering, St. Joseph Engineering College, Mangalore,

India

[3] Department of Electronics and Computer Engineering, Ngee Ann Polytechnic, Singapore, 599489

[4]Department of Biomedical Engineering, SIM University, Singapore.

[5] Diabetes Health Districts 8-9-10 Diabetes Unit ASL TO1 di Torino, Torino, Italy

[6] "Un passo insieme" ONLUS Foundation, Valdellatorre, Torino, Italy

Corresponding Author:

Professor Filippo Molinari, PhD

Biolab - Department of Electronics and Telecommunications - Politecnico di Torino

Corso Duca degli Abruzzi, 24; 10129 Torino, Italy;

(e-mail: filippo.molinari@polito.it, tel: +39 11 564 4135)

Abstract

Type 2 diabetes is a metabolic disorder that may cause major problems to several physiological systems. Exercise has proven to be very effective in the prevention, management and improvement of this pathology in patients.Muscle metabolism is often studied with Near-infrared spectroscopy (NIRS), a noninvasive technique that can measure changes in the concentration of oxygenated (O2Hb) and reduced hemoglobin (HHb) of tissues. These NIRS signals are highly non-stationary, non-Gaussian and nonlinear in nature.

The Empirical Mode Decomposition (EMD) is used as a nonlinear adaptive model to extract information present in the NIRS signals. NIRS signals acquired from the tibialis anterior muscle of controls and Type 2 diabetic patients are processed by EMD to yield three intrinsic mode functions (IMF). The Sample Entropy (SE), Fractal Dimension (FD), and Hurst Exponent (HE) are computed from these IMFs. Subjects are monitored at the beginning of the study and after one year of a physical training programme.

Following the exercise programme, we observed an increase in the SE and FD and a decrease in the HE in all diabetic subjects. Our results shows the influence of physical exercise program in improving muscle performance and muscle drive by the central nervous system in the patients. A multivariate analysis of variance performed at the end of the training programme also indicated that the NIRS metabolic patterns of controls and diabetic subjects are more similar than at the beginning of the study.

Hence, the proposed EMD technique applied to NIRS signals may be very useful to gain a non-invasive understanding of the neuromuscular and vascular impairment in diabetic subjects.

1. Introduction and background

Type 2 diabetes mellitus is a commonly diffused pathology and it is increasing at an alarming rate. According to Adeghate et. al (1) diabetes will affect 300 million people by 2025 and Kaul et al. (2) state that 97% of patients will suffer from type 2 diabetes who have insulin resistance and insulin deficiency. Moreover, the global prevalence of diabetes is not limited to only industrialized or only emerging countries, but is rather increasing in both. Type 2 diabetes mellitus is associated with cardiovascular diseases (3), neuropathy (4), peripheral vascular insufficiency (5), lung dysfunction (6), and retinopathy (7).

Various studies have shown how a specific change in life-style, such as diet, weight loss, and exercise, are very effective in the prevention, management and improvement of this pathology in patients (8). Exercise in particular has shown promising results, improving vascular protection and insulin resistance (9) and reducing the negative effects of neuropathy (10).

Exercise has positive effects on different aspects of muscular action, and it can often be difficult to correctly assess the actual improvement that exercise has on type 2 diabetes patients. Bagai et al. (11) analyzed the variation of the surface myoelectric signal (EMG – electromyogram) in diabetes patients as a result of polyneuropathy. Other experiments have shown how the spatial distribution of the EMG of the vastus lateralis is different when comparing patients with healthy controls (12). However, two very important factors in the assessment of diabetic patients, the local muscular metabolic rate and the efficiency of the peripheral muscle vascularization, cannot be fully captured by the EMG despite their importance in the determination of muscle contraction and performance.

Near infrared spectroscopy (NIRS) has been used to monitor patients suffering from lower-extremity arterial disease (13) and diabetes (14). This technique is portable, non-invasive, and low-cost, making it easy for patients to use during exercise and rest. Electrochemical systems based on reverse iontophoresis are more accurate than NIRS systems in the glucose concentration monitoring (15); however NIRS systems are a good choice for this study as they are less invasive and real-time. The light sources of the NIRS system emit electromagnetic radiation and the absorption of light of different tissues at certain wavelengths allows measuring the chromophore concentration in the observed tissue. Two main chromophores that are present in

human tissue are oxygenated and reduced haemoglobin. Haemoglobin shows two different absorption peaks in the NIR spectrum: at 850-900 nm if in its oxygenated (i.e. oxidized) form (for simplicity, indicated by O2Hb from here on out), and at 730-750 nm if in its deoxygenated (i.e. reduced) form (HHb). These different properties, the concentration of each haemoglobin type, can be easily estimated by irradiating the tissue at two separate wavelengths (16). Features extracted from NIRS recordings of diabetics during exercise have proven to be useful to assess the neuromuscular and peripheral pattern (17).

NIRS signals can typically tend to present a marked non-stationary nature (17) (18). Very low frequency components associated with long-term regulatory mechanisms makes the baseline of the NIRS signals vary (19), and the signal power depends on the local metabolic rate and oxygen consumption. Moreover, NIRS signals present a time dependent average value, which reflects the concentration changes of the chromophore. Due to the nonlinear nature of the NIRS signal, linear, frequency and time-frequency domain methods may not be able to fully extract the small variations from the signals, whereas nonlinear interrelationships in the NIRS data can provide more accurate information. Previous studies have demonstrated how non-stationary and nonlinear methods are needed to analyze glucose levels (20) and insulin sensitivity (21) of diabetic subjects. Also, bispectral analysis has been used for epilepsy diagnosis (22) (23), sleep stages (24), cardiac abnormalities (25), EEG signals (26), and myoelectric signals (27). Moreover, the entropy analysis of NIRS signals, coupled with unsupervised clustering, has proven to highlight the changes in muscle contraction performance of diabetic patients as a consequence of exercise (28). The results of these specific types of analysis can sometimes be difficult to interpret and understand. In a previous work, we analyzed the NIRS signals recorded during muscle contractions of diabetic patients by using higher-order spectra, bispectral and sample entropies (28). We demonstrated that physical activity improved the muscle metabolism and, specifically, that the NIRS pattern of diabetic subjects after physical activity is close to the healthy controls. Our previous study had two major limitations. Methodological point of view, we did not investigate the nonlinear architecture of the NIRS signals. Also from a physiological point of view, we only analyzed the NIRS signals recorded during muscle activation, but not during resting (*i.e.* baseline conditions).

A simple, adaptive and local structure based, nonlinear measure, such as the empirical mode decomposition (EMD), can instead provide more intuitive understanding of the data. In this paper, we show

how the EMD analysis of NIRS signals can highlight the changes in muscle contraction performance of diabetic patients. We tested a group of subjects with type 2 diabetes who underwent a year of an exercise programme, specifically adapted to their age and physical condition. NIRS captured the changes in the metabolic aspect of muscle contraction and showed that after the one-year training programme, the muscle metabolic pattern of diabetics as found with EMD is similar to those of healthy controls.

2. Patient demographics and experimental setup

Twenty-four diabetes type 2 subjects were enrolled in the study along with sixteen healthy controls. The diabetic patients were non-consecutive and enrolled with the following inclusion criteria: age > 50 years; body mass index (BMI) between 18 and 23 kg/m^2, and diabetes onset at least 10 years before the study. Exclusion criteria were only related to possible physical or mental states that precluded the possibility of following a long physical activity programme. All the diabetic subjects underwent daily physical activity for one year. Of the 24 patients, the physical activity for 15 of the patients was an adapted physical training (APT) program (age: 66.7 ± 5.7 years), whereas the remaining 9 practiced fit walking (FW) (age: 66.0 ± 6.2 years). APT consisted in low load exercised for the lower and upper limb muscles, whereas FW consisted in walking at a constant pacing. Expert exercise physiologists and therapists followed each patient and set the intensity of each exercise. For the control group, the 16 healthy subjects were age-matched (age: 65.3 ± 3.9 years) and physically active. Table 1 summarizes the patient demographics, including also their glycated haemoglobin (HbA1c) level (29) and the Neuropathy Disability Score (NDS) (4). The Gradenigo Hospital institutional review board, where all tests were performed, gave the approval for this study. All of the patients were informed about the study methods and goals and signed an informed consent before the test.

The NIRO300 NIRS system (Hamamatsu Photonics, Japan) was used to record the NIRS signals of each patient before, during, and after the physical exercise. The NIRO300 emitting probe consists of four laser diodes at the following wavelengths: 775 nm, 813 nm, 853 nm, and 910 nm. In order to convert the light absorbance into concentration, the NIRS systems used the modified Beer-Lambert law (30). This law empirically models the light absorption in a highly scattering medium:

$$A = log\left(\frac{I_0}{I}\right) = \alpha \cdot c \cdot B \cdot d + G \qquad (1)$$

where A is light attenuation, I_0 the emitted light intensity, I the received intensity, c the concentration of a chromophore (in our study oxygenated or reduced hemoglobin), α is the extinction coefficient of the chromophore at a given wavelength, and d is the source-receiver distance. Scattering causes photon loss (*i.e.* photons that are emitted by the source but that are scattered so that they do not reach the receiver) and an increase in the path the photons travel before reaching the receiver. In eq. (1), G models the photon loss and B the path increase (called differential pathlength factor – DPF). Since photon loss cannot be quantified it is not possible to measure the absolute light attenuation. Assuming G as constant, the modified Beer-Lambert law is rewritten as:

$$\Delta A = log\left(\frac{I_0}{I}\right) = \alpha \cdot \Delta c \cdot B \cdot d \qquad (2)$$

where ΔA is the change in light attenuation caused by the change Δc in the chromophore concentration. We set a value of B equal to 5 (31). Equation (2) is relative to a single wavelength, thus by combining different wavelengths it is possible to measure the concentration of different chromophores.

In this study, we observed the changes in the concentration of four NIRS signals: the oxygenated haemoglobin (O2Hb), deoxygenated haemoglobin (HHb), the tissue oxygenation index (TOI), and the normalized tissue haemoglobin index (THI). The TOI is defined as the ratio between oxygenated haemoglobin and total haemoglobin (16), whereas the THI is defined as the relative concentration of total haemoglobin (16).

The emission probe was positioned along the muscle belly of the patient's left tibialis anterior muscle, whereas the detection probe was placed 4 cm away and in the distal direction of the muscle fibers (i.e. towards the subject's ankle and away from the probe). The sampling frequency of the NIRS signals was equal to 2Hz. The experiment lasted a total of 7 min, divided into three separate steps: (i) rest for 1 minute (baseline), (ii) 3 minutes of ankle flex-extensions (exercise), and (iii) 3 minutes of recovery (rest). All the subjects were tested separately and in random order.

Figure 1 shows typical O2Hb and HHb NIRS signals during the experiment. The O2Hb concentration decreases during muscle contraction, due to oxygen consumption and decreased blood inflow, whereas the concentration of HHb increases due to a reduced washout and a local accumulation of carbon dioxide (13).

3. Methodology

This section discusses the decomposition of NIRS signals using the Empirical Mode Decomposition (EMD) to obtain three intrinsic mode functions (IMFs). In this section we briefly explain the Higuchi fractal dimension (FD), sample entropy (SE) and the Hurst exponent (HE) applied on IMFs to study the characteristics of the NIRS signals.

3.1 Empirical Mode Decomposition (EMD)

The empirical mode decomposition is an adaptive, data dependent and direct method of time-frequency decomposition. Unlike any other time-frequency transform, it does not assume linearity as a requirement. The method is also called the Hilbert Huang transform (HHT)(32). Any complicated dataset can be decomposed into a set of a few intrinsic mode functions (IMFs) that have well defined proper rotation components. The decomposition of the given data into a set of IMFs is based on the data's local characteristics of time and scale. The IMFs derived from the given signal satisfy two basic assumptions: (1) In the entire data segment, the total number of extrema (both maxima and minima) are equal to or differ at most by one with the number of zero crossings; (2) The mean value of the envelope given by the local minima and local maxima must be zero. The EMD algorithm is provided below as a step by step procedure (32).

Step 1: Let $x(t)$ be the given signal. The local minima and local maxima are to be extracted. A cubic spline curve is used to connect all the local maxima, providing the upper envelope. Let this curve be $x_u(t)$. The local minima are connected in the same way with a cubic spline curve and name that curve as $x_l(t)$. The mean envelope between the upper and lower envelopes is computed as:

$$m_1(t) = \frac{x_u(t) + x_l(t)}{2} \qquad (3)$$

Then the first IMF is derived as:

$$h_1(t) = x(t) - m_1(t) \qquad (4)$$

This procedure is called as *sifting*.

Step 2: The derived first IMF $h_1(t)$ is considered as the signal and its lower and upper envelopes are computed. From this mean envelope, the following is computed to provide:

$$h_1 - m_{11} = h_{11} \qquad (5)$$

Step 3: This process is repeated k times until h_{1k} is an IMF:

$$h_{1(k-1)} - m_{1k} = h_{1k} \qquad (6)$$

This procedure is continued until the normalized standard deviation (NSD in the following equation) between the two consecutive IMFs is less than 0.2 or 0.3:

$$NSD = \frac{\sum_{t=1}^{T} \left| h_{1(k-1)}(t) - h_{1k}(t) \right|}{h_{1(k-1)}^2(t)} \qquad (7)$$

The final IMF is $c_1 = h_{1k}$. Then $x(t) - c_1 = r_1$ is called the residue signal and represents the trend of the data time series. The original signal can be represented in terms of the linear combination of IMF and the residue as:

$$x(t) = \sum_{m=1}^{M} h_m(t) + r_M(t) \qquad (8)$$

where M denotes the total number of IMFs, h_m is the m-th IMF and r_M is the residue signal.

For each IMF we calculated three descriptors related to the complexity of the signals, which are: the Higuchi

Fractal Dimension (FD); the Hurst Exponent (HE) and the Sample Entropy (SE).

3.2 Higuchi Fractal Dimension (FD)

The Higuchi's algorithm is a method for the calculation of the fractal dimension D of a time series (33)

(34). This algorithm is based on a measure of length, called $L(k)$, of the time series by using a segment of k

samples as a unit if the length scales as:

$$L(k) \sim k^{-D} \qquad (9)$$

An increase in the Higuchi FD reveals a more complex and nonlinear system. Hence, in our study, since

diabetes causes a selective loss of muscle fibers and a consequent reduction of the system complexity, higher

values of FD of diabetic patients could indicate a muscle behavior similar to healthy controls.

3.3 Sample Entropy (SE)

Sample entropy is an embedding entropy which directly uses the time series instead of making use of

probability values (35). Let $h_i(n), n = 1, 2, 3, ..., N$ be the original time series. New vector sequences of size

m are generated from $u(1)$ to $u(N-m+1)$. These derived vector sequences are defined as,

$u(n) = \{h_i(n), h_i(n+1), ..., h_i(n+m-1)\}$ (35). The specified length m is named the embedding

dimension. The distance $d(u(n_1), u(n_2))$ between the two vectors $u(n_1)$ and $u(n_2)$ is determined as (35):

$$d(u(n_1), u(n_2)) = \max\{|u(n_1+n_3) - u(n_2+n_3)|\}, 0 \le k \le m-1 \qquad (10)$$

where n_3 is an index. Therefore, we can define the probability of locating another vector not beyond the

distance r from the vector $u(n_1)$ as (35):

$$C_{n_1}^n(r) = \frac{\{\text{The number of } n_2, n_2 \ne n_1, n_2 \le N-n+1 \text{ such that } d(u(n_1), u(n_2)) \le r\}}{N-n+1} \qquad (11)$$

We can calculate,

$$\phi^m(r) = (N-n+1)^{-1} \sum_{n_1=1}^{N-n+1} C_{n_1}^n(r) \qquad (12)$$

The sample entropy is determined as:

$$SE(n, r, N) = -ln\left[\frac{\phi^n(r)}{\phi^{n+1}(r)}\right] \qquad (13)$$

The variable r is the tolerance of accepting analogous patterns between two segments.

3.4 Hurst Exponent (HE)

The Hurst exponent measures the presence or absence of long-range in a signal, along with the dependence degree[36]. For each observation, the *mean* of the time series is computed, along with the *mean* centered series, obtained by subtracting the *mean* from the series, and the cumulative deviation of the series from the *mean*, obtained by summing up the mean centered values. The Hurst Exponent therefore quantifies the *smoothness* of a fractal time series, and can be defined as:

$$HE = log(R/S)/log(T) \qquad (15)$$

Where R represents the range, which is the difference between the maximum value of the cumulative deviation and the minimum value of the cumulative deviation, and S is the standard deviation of the *mean* centered values. T is the duration of the sample of data. Higher HE values correspond to smoother fractal time series, and therefore to less complex systems.

Hence, for each subject we measured the Higuchi Fractal Dimension (FD), the Hurst Exponent (HE) and the Sample Entropy (SE) for each of the three intrinsic mode functions of the O2Hb, HHb, TOI, and THI signals. So, we obtained 36 measurements for each subject. Since we tested the same subjects in two different moments (*i.e.* baseline and during exercise), and hence total number of 72 variables associated to each subject. Therefore, we have a data matrix of 40 (number of tested subjects) by 72 (number of variables) describing the initial conditions before the physical activity programme onset, and another matrix of same dimensions that we obtained one year after, at the end of the activity programme.

3.5 Statistical Analysis

The grouped values are represented by average value ± SD. A statistical analysis of the average values is performed by using the Student's *t*-test, after having tested for normality of the data by the Kolmogorov–

Smirnov test. The significance level is set to 0.9, thus allowing a first-species error of 0.1. The multivariate data matrix is analyzed by using the one-way multivariate ANOVA (MANOVA), which is applied on the data before and after the physical activity. The MANOVA represents the subjects in function of the so-called canonical variables, which are linear combination of the original features. The first canonical variable is the one explaining the maximum variance of the original feature set, the second is the one explaining the maximum residual variance, and so on. We will consider the representation of the subjects in function of the first two canonical variables, which are the most meaningful. The original features that have the highest coefficients in the canonical variables are considered the more discriminant to assess the changes induced by the physical activity and captured by NIRS.

4. Results

In this study, we applied the EMD on NIRS signals acquired from healthy and diabetic subjects before, during, and after muscle contraction, and then we computed the SE, FD and HE on the first three intrinsic mode functions (IMFs). The purpose of this work is to assess the metabolic muscular pattern differences in patients before and after physical training.

First of all, we compared the EMD derived parameters for the three subject groups before and after physical training. Tables 2.a, 2.b and 2.c show the data for the three IMFs of the O2Hb, HHb, TOI and THI signals obtained before and after the training period *during exercise* for the healthy controls, the fit-walking patients, and the adapted physical training patients, respectively. It can be observed that there is no significant changes in the parameter values as a consequence of the physical activity, except for the HE of the first IMF of the TOI signal. Hence, the changes in the oxygenation signals of the healthy controls are absent. The change in the HE of the TOI reflects the change in the HHb signal, since the TOI value strongly depends on the HHb concentration changes. It demonstrates that physical activity has no significant effect on the metabolic pattern of the control subjects, who are physically active even when enrolled in the study. It can be observed in Tables 2.b and 2.c that both the fit walking and the adapted physical training patient groups show an increase in the SE after the physical activity, for all IMFs of the NIRS signals. Such increase

is statistically significant for the third IMF of the O2Hb signal and the second IMF of the HHb signal for the fit walking group, whereas for the APT group, this increase is statistically significant for the first IMF of the HHb and TOI signals, and the second IMF of the O2Hb and THI signals. The HE decreases after the physical training, which is statistically significant for the third IMF of the O2Hb signal for the fit walking patient group. In the APT patient group, the HE difference for the second IMF of the HHb and TOI signals, and for the third IMF of the TOI signal is statistically significant. The FD shows values that are quite similar for both before and after the physical training; however, a statistically significant increase can be observed in the fit walking patient group for the second and third IMF of the THI signal. A statistically significant difference for the first and second IMF of the O2Hb signal and for the third IMF of the HHb signal can be seen in the APT patient group.

Similarly, Tables 3.a, 3.b and 3.c show the results of three IMFs using the O2Hb, HHb, TOI and THI signals obtained before and after the training period *during baseline* for the healthy controls, the fit-walking patients, and the adapted physical training patients, respectively. Controls did not show remarkable changes in the parameters during baseline conditions, except for the case of the FD and HE of the second and third IMF of the HHb signal, respectively, and the SE of the third IMF of the TOI signal (Table 3.a). The diabetic subjects of the fit walking group exhibited an increase in the SE for the O2Hb, THI and TOI signals. The HE increased in the third IMF of the O2Hb and of the THI signals, but decreased in the first and third IMF of the TOI signal and in the first IMF of the HHb signal. No significant changes are observed for the FD (Table 3.b). Opposite to the fit walking group, Table 3.c shows that the HE decreased in the IMFs of the O2Hb and THI signals relative to the diabetic subjects who performed APT, and increased in the third IMF of the TOI signal. The HHb signal showed unclear changes, because the HE decreased in the first IMF and increased in the third IMF. The SE increased slightly in the third IMF of the TOI signal, whereas the FD did not show significant changes. Therefore, even if both groups of diabetic subjects showed changes in their NIRS pattern in resting condition, such changes are overall opposite and dependent on the kind of physical training performed.

The previous results compared the NIRS metabolic pattern of the subjects belonging to the same group before and after physical training. To compare the effect of training among the groups, we performed the

one-way MANOVA analysis considering the group as the independent variable. Figure 2 is relative to the *baseline*, and it represents the subjects in the plane of the first and second canonical variable of the MANOVA before (left panel) and after (right panel) physical training. It can be noticed that, after training, the subjects are closer than at the beginning, showing that diabetic subjects became more similar to controls. Before training, the dimension of the MANOVA is 2 (*p* values equal to 10^{-5} and 0.0483), thus it is possible to reject the hypothesis that the subjects belonged to the same group. After training the dimension is equal to 1 (*p* values equal to 0.0238 and 0.9706), thus indicating that only two groups can be distinguished (APT from controls plus FW). Similarly, figure 3 shows the subjects in function of the canonical variables during *exercise*. Before the training (left panel) the dimension of the MANOVA is equal to 1 (*p* values equal to 10^{-5} and 0.1522), and the subjects did not belong to the same group. After the training (right panel) the dimension lowered to 0 (*p* values equal to 0.2037 and 0.5361), thus it is not possible to reject the hypothesis that the subjects belonged to the same group. In other words, during exercise and after training, all the subjects (diabetic and controls) showed substantially the same NIRS pattern. Finally, Table 4 reports the five most discriminant variables among groups for the four conditions (baseline before/after and exercise before/after).

5. Discussion

Our obtained results demonstrate that physical activity (either APT or FW) increased the SE and FD, and decreased the HE of the NRS signals during excercise. When comparing the subjects before and after the training, the increase in SE is more evident on the O2Hb and TOI signals, which directly reflect the oxygenation status of the muscle fibers (13, 37). Previous studies already showed that accurately measuring the improvement in the overall neuromuscular status of the subjects is a significant step (28).

We have also performed multivariate analysis of variance (MANOVA) test on the dataset. We separately analyzed the baseline condition and during exercise. During baseline, when the muscle is not active, the changes in the concentration of the chromophores are mainly due to vascular and neurological impairment, whereas during exercise the muscle metabolism and composition plays a role. We observe that at the beginning of the study there is a neat separation between the groups in baseline conditions, while this

difference decreased after one year of physical training (fig. 2). The most discriminant features among the groups are relative to either the HHb or the TOI signal. Particularly, the FD of the first IMF of the HHb signal is the most important feature to distinguish the subjects (Table 4, first row). Higher values of FD describe more complex and variable patterns, which correspond to a healthy and well functioning neuromuscular system (12, 28). Also, previous studies related to the central nervous system demonstrated that, carbon dioxide is the chromophore whose changes are more indicative of the status of the system (28, 38). During muscle contraction (fig. 3), muscle metabolism, muscle fiber conduction velocity, and venous outflow play a major role and the effect of training is even more evident. After training, it is not possible to reject the hypothesis that all subjects belong to the same group. Even during exercise, the most discriminant variables are all related to the first IMF of the HHb signal (Table 4, the two rightmost columns).

We have taken care to avoid possible biases due to degradating of the optical instrumentation. The NIRO300 system has an emitting probe consisting of laser diodes. We have calibrated the system before each acquisition by using the optical phantom provided by the manufacturer in order to exclude the degradation of the laser source., We did not observe any failure or warning messages in the calibration procedures.

From a clinical point of view, the use of non-linear features extracted from the NIRS signals during a muscle contraction yielded a better assessment of the neuromuscular system of the subjects. The overall system complexity can be adequately quantified by using FD, HE, and SE. The EMD time-frequency analysis can extract the inner nonstationarity present in the NIRS signals. In fact, traditional spectral techniques cannot provide adequate information on this kind of signals, because of a lack of spectral resolution. The EMD is a nonlinear method which can be used for processing NIRS signals and it does not require stationarity and linearity conditions of the signals.

A limitation of the study is the impossibility of assessing separately the neurological and vascular impairment of diabetic subjects. More studies are needed to understand vascular impairments (mainly in the arterial compartment), and impact of the EMG signal due to dynamic contractions. An important development, connected to the, is the investigation of the recovery phase (fig. 1, last part of the signals). During recovery the NIRS signals can be approximated by exponential functions (13), and it is shown that

longer recovery time is associated to a peripheral artery disease with claudication (13). However, the estimation of the exponential time constant may be difficult in certain conditions, because of the low signal-to-noise ratio typical of NIRS recording. In our experience, often the recovery time did not produce significant results. However, since the NIRS signal has overt variations during recovery, dedicated procedures must be developed. In this work, we did not analyze the recovery phase. A second limitation of this study is the absence of a group of diabetic patients who did not follow any physical activity programme. Such control group may be useful to better understand the reasons why physical activity caused this overt effect on the NIRS signals architecture.

6. Conclusions

NIRS signals can be reliably used to assess the neuromuscular and metabolic state of muscles in type 2 diabetic patients. The subtle changes in NIRS signals must be captured accurately and robust processing techniques must be adopted, because of their non-stationary and non-linear nature. In this paper, various nonlinear features are extracted from the IMFs of the EMD method applied on muscular NIRS signals recorded during baseline and during ankle movement. Our results clearly indicate that diabetic subjects who underwent one year of physical training improved their NIRS pattern and increased the FD and SE, while the HE is reduced. These results document that the NIRS metabolic pattern of diabetic patients becomes more complex and this is a clinically positive results, because complexity is a condition typical of healthy subjects. Even though more studies are needed, EMD applied to NIRS signals is very useful to gain a non-invasive deeper understanding of the neuromuscular and vascular impairment of diabetic subjects.

REFERENCES

1.   Adeghate E, Schattner P, Dunn E. An update on the etiology and epidemiology of diabetes mellitus. Annals of the New York Academy of Sciences. 2006;1084:1-29.
2.   Kaul K, Tarr JM, Ahmad SI, Kohner EM, Chibber R. Introduction to diabetes mellitus. Advances in experimental medicine and biology. 2012;771:1-11.
3.   Van Dieren S, Beulens JWJ, Kengne AP, Peelen LM, Rutten GEHM, Woodward M, et al. Prediction models for the risk of cardiovascular disease in patients with type 2 diabetes: A systematic review. Heart. 2012;98(5):360-9.
4.   Vileikyte L, Leventhal H, Gonzalez JS, Peyrot M, Rubin RR, Ulbrecht JS, et al. Diabetic peripheral neuropathy and depressive symptoms: The association revisited. Diabetes Care. 2005;28(10):2378-83.
5.   Huysman F, Mathieu C. Diabetes and peripheral vascular disease. Acta Chirurgica Belgica. 2009;109(5):587-94.
6.   Klein OL, Krishnan JA, Glick S, Smith LJ. Systematic review of the association between lung function and Type 2 diabetes mellitus. Diabetic Medicine. 2010;27(9):977-87.
7.   Prabhu S, Chakraborty C, Banerjee RN, Ray AK. Study of retinal biometric systems with respect to feature classification for recognition and diabetic retinopathy. Journal of Medical Imaging and Health Informatics. 2011;1(2):97-106.
8.   Imam K. Management and treatment of diabetes mellitus. Advances in experimental medicine and biology. 2012;771:356-80.
9.   Utsunomiya K. Treatment strategy for type 2 diabetes from the perspective of systemic vascular protection and insulin resistance. Vascular Health and Risk Management. 2012;8(1):429-36.
10.   Karayannis G, Giamouzis G, Cokkinos DV, Skoularigis J, Triposkiadis F. Diabetic cardiovascular autonomic neuropathy: Clinical implications. Expert Review of Cardiovascular Therapy. 2012;10(6):747-65.
11.   Bagai K, Wilson JR, Khanna M, Song Y, Wang L, Fisher MA. Electrophysiological patterns of diabetic polyneuropathy. Electromyography and Clinical Neurophysiology. 2008;48(3-4):139-45.
12.   Watanabe K, Miyamoto T, Tanaka Y, Fukuda K, Moritani T. Type 2 diabetes mellitus patients manifest characteristic spatial EMG potential distribution pattern during sustained isometric contraction. Diabetes research and clinical practice. 2012;97(3):468-73.
13.   Comerota AJ, Throm RC, Kelly P, Jaff M. Tissue (muscle) oxygen saturation (StO2): A new measure of symptomatic lower-extremity arterial disease. Journal of Vascular Surgery. 2003;38(4):724-9.
14.   De Blasi RA, Luciani R, Punzo G, Arcioni R, Romano R, Boezi M, et al. Microcirculatory changes and skeletal muscle oxygenation measured at rest by non-infrared spectroscopy in patients with and without diabetes undergoing haemodialysis. Critical care (London, England). 2009;13 Suppl 5.
15.   Chang L, Liu C, He Y, Xiao H, Cai X. Small-volume solution current-time behavior study for application in reverse iontophoresis-based non-invasive blood glucose monitoring. Sci China Chem. 2011;54(1):223-30.
16.   Elwell CE, Cooper CE. Making light work: Illuminating the future of biomedical optics. Philosophical Transactions of the Royal Society A: Mathematical, Physical and Engineering Sciences. 2011;369(1955):4358-79.
17.   Molinari F, Rosati S, Liboni W, Negri E, Mana O, Allais G, et al. Time-frequency characterization of cerebral hemodynamics of migraine sufferers as assessed by NIRS signals. Eurasip Journal on Advances in Signal Processing. 2010;2010.
18.   Molinari F, Liboni W, Grippi G, Negri E. Relationship between oxygen supply and cerebral blood flow assessed by transcranial Doppler and near - Infrared spectroscopy in healthy subjects during breath - Holding. Journal of NeuroEngineering and Rehabilitation. 2006;3.
19.   Obrig H, Neufang M, Wenzel R, Kohl M, Steinbrink J, Einhaupl K, et al. Spontaneous low frequency oscillations of cerebral hemodynamics and metabolism in human adults. NeuroImage. 2000;12(6):623-39.
20.   Khovanova NA, Khovanov IA, Sbano L, Griffiths F, Holt TA. Characterisation of linear predictability and non-stationarity of subcutaneous glucose profiles. Computer Methods and Programs in Biomedicine. 2013;110(3):260-7.
21.   Yates JWT, Watson EM. Estimating insulin sensitivity from glucose levels only: Use of a non-linear mixed effects approach and maximum a posteriori (MAP) estimation. Computer Methods and Programs in Biomedicine. 2013;109(2):134-43.

22.   Chua KC, Chandran V, Rajendra Acharya U, Lim CM. Analysis of epileptic EEG signals using higher order spectra. Journal of Medical Engineering and Technology. 2009;33(1):42-50.

23.   Acharya UR, Sree SV, Suri JS. Automatic detection of epileptic eeg signals using higher order cumulant features. International Journal of Neural Systems. 2011;21(5):403-14.

24.   Acharya UR, Chua ECP, Chua KC, Min LC, Tamura T. Analysis and automatic identification of sleep stages using higher order spectra. International Journal of Neural Systems. 2010;20(6):509-21.

25.   Chua KC, Chandran V, Acharya UR, Lim CM. Cardiac state diagnosis using higher order spectra of heart rate variability. Journal of Medical Engineering and Technology. 2008;32(2):145-55.

26.   Hosseinifard B, Moradi MH, Rostami R. Classifying depression patients and normal subjects using machine learning techniques and nonlinear features from EEG signal. Computer Methods and Programs in Biomedicine. 2013;109(3):339-45.

27.   Zazula D, Holobar A. An approach to surface EMG decomposition based on higher-order cumulants. Computer Methods and Programs in Biomedicine. 2005;80(SUPPL. 1):S51-S60.

28.   Molinari F, Acharya UR, Martis RJ, De Luca R, Petraroli G, Liboni W. Entropy analysis of muscular near-infrared spectroscopy (NIRS) signals during exercise programme of type 2 diabetic patients: quantitative assessment of muscle metabolic pattern. Computer methods and programs in biomedicine. 2013;112(3):518-28.

29.   Weykamp C, John WG, Mosca A, Hoshino T, Little R, Jeppsson JO, et al. The IFCC reference measurement system for HbA1c: A 6-year progress report. Clinical Chemistry. 2008;54(2):240-8.

30.   Boas DA, Gaudette T, Strangman G, Cheng X, Marota JJ, Mandeville JB. The accuracy of near infrared spectroscopy and imaging during focal changes in cerebral hemodynamics. Neuroimage. 2001;13(1):76-90.

31.   Duncan A, Meek JH, Clemence M, Elwell CE, Tyszczuk L, Cope M, et al. Optical pathlength measurements on adult head, calf and forearm and the head of the newborn infant using phase resolved optical spectroscopy. Physics in medicine and biology. 1995;40(2):295-304.

32.   Huang NE, Shen Z, Long SR, Wu MC, Shih HH, Zheng Q, et al. The empirical mode decomposition and the Hilbert spectrum for nonlinear and non-stationary time series analysis. Proceedings of the Royal Society of London Series A: Mathematical, Physical and Engineering Sciences. 1998;454(1971):903-95.

33.   Higuchi T. Approach to an irregular time series on the basis of the fractal theory. Physica D: Nonlinear Phenomena. 1988;31(2):277-83.

34.   Higuchi T. Relationship between the fractal dimension and the power law index for a time series: a numerical investigation. Physica D: Nonlinear Phenomena. 1990;46(2):254-64.

35.   Richman JS, Moorman JR. Physiological time-series analysis using approximate entropy and sample entropy. American Journal of Physiology-Heart and Circulatory Physiology. 2000;278(6):H2039-H49.

36.   Hurst HE. Long-term storage capacity of reservoirs. Transactions of the American Society of Civil Engineers. 1951;116:770-808.

37.   Bhambhani Y, Buckley S, Susaki T. Muscle oxygenation trends during constant work rate cycle exercise in men and women. Medicine and Science in Sports and Exercise. 1999;31(1):90-8.

38.   Molinari F, Simonetti V, Franzini M, Pandolfi S, Vaiano F, Valdenassi L, et al. Ozone autohemotherapy induces long-term cerebral metabolic changes in multiple sclerosis patients. International journal of immunopathology and pharmacology. 2014;27(3):379-89.

Tables

Table 1.

Demographics of the patients and of the healthy controls

	APT group (15 patients)	FW group (9 patients)	Controls (16 subjects)
Age (years)	66.7 ± 5.7	66.0 ± 6.2	65.2 ± 3.9
Males	10	14	8
HbA1c (%)	7.8 ± 1.0	7.4 ± 0.9	5.2 ± 1.6*
HbA1c (mmol/mol)	62 ± 14	57 ± 14	33 ± 6*
BMI (km/m2)	19.3 ± 2.2	20.2 ± 1.9	19.5 ± 1.5
Duration diabetes (years)	19.0 ± 9.9	18.7 ± 10.1	-
Neuropathy disability score (NDS)	2.04 ± 1.92	1.82 ± 1.87	-

*The values are statistically different from those of patients ($p < 0.1$)

Table 2.a – EMD derived features for controls during exercise.

Signal	IMF	Features	Pre	Post	p-Value
O2Hb	IMF1	FD	2.0514 ± 0.0387	2.0404 ± 0.0271	0.4532
		HE	0.1985 ± 0.1347	0.2592 ± 0.0853	0.2151
		SE	2.1307 ± 0.0620	2.1225 ± 0.1097	0.7660
	IMF2	FD	1.8804 ± 0.1003	1.8582 ± 0.1139	0.4723
		HE	0.3385 ± 0.1353	0.2798 ± 0.1526	0.3103
		SE	2.1331 ± 0.0700	2.0900 ± 0.1068	0.1746
	IMF3	FD	1.3353 ± 0.1262	1.3296 ± 0.1644	0.9089
		HE	0.5084 ± 0.1015	0.4750 ± 0.1619	0.5312
		SE	1.8720 ± 0.3131	1.9201 ± 0.3217	0.6294
HHb	IMF1	FD	2.0524 ± 0.0355	2.0407 ± 0.0275	0.4061
		HE	0.2565 ± 0.1213	0.2936 ± 0.1130	0.3757
		SE	2.1200 ± 0.1069	2.1445 ± 0.1191	0.5949
	IMF2	FD	1.8822 ± 0.0736	1.8939 ± 0.0663	0.7024
		HE	0.3090 ± 0.1064	0.2909 ± 0.1045	0.6477
		SE	2.1106 ± 0.0984	2.0680 ± 0.1072	0.2341
	IMF3	FD	1.3733 ± 0.1071	1.3786 ± 0.1249	0.8969
		HE	0.4651 ± 0.1263	0.5078 ± 0.1561	0.4630

		SE	1.9565 ± 0.2580	2.0467 ± 0.1828	0.2914
THI	IMF1	FD	2.0594 ± 0.0414	2.0421 ± 0.0307	0.2187
		HE	0.2081 ± 0.0909	0.2769 ± 0.1206	0.1053
		SE	2.1105 ± 0.0678	2.0897 ± 0.1382	0.5357
	IMF2	FD	1.8988 ± 0.0687	1.8948 ± 0.0616	0.8595
		HE	0.2384 ± 0.0922	0.2658 ± 0.1233	0.5300
		SE	2.1271 ± 0.0753	2.0767 ± 0.1428	0.2688
	IMF3	FD	1.4508 ± 0.1197	1.4438 ± 0.1126	0.8364
		HE	0.3882 ± 0.1206	0.4132 ± 0.1003	0.5250
		SE	2.0702 ± 0.1369	2.0493 ± 0.1540	0.6644
TOI	IMF1	FD	2.0455 ± 0.0161	2.0367 ± 0.0184	0.1929
		HE	0.2395 ± 0.0975	0.2928 ± 0.0518	0.0781*
		SE	2.1530 ± 0.0905	2.1572 ± 0.0774	0.9003
	IMF2	FD	1.9132 ± 0.0327	1.8962 ± 0.0357	0.1526
		HE	0.2491 ± 0.1311	0.2761 ± 0.0671	0.4058
		SE	2.1365 ± 0.0726	2.1389 ± 0.1379	0.9533
	IMF3	FD	1.4353 ± 0.0760	1.4024 ± 0.1074	0.2771
		HE	0.4076 ± 0.1381	0.4310 ± 0.1321	0.6133
		SE	2.0309 ± 0.1935	2.0905 ± 0.1225	0.1579

Table 2.b – EMD derived features for diabetic subjects who performed fit walking during exercise.

Signal	IMF	Features	Pre	Post	p-Value
		Fit Walking exercise			
O2Hb	IMF1	FD	2.0246 ± 0.0741	2.0469 ± 0.0394	0.2874
		HE	0.2701 ± 0.1929	0.2604 ± 0.0857	0.8701
		SE	1.9663 ± 0.4705	2.0700 ± 0.2246	0.4666
	IMF2	FD	1.8275 ± 0.1287	1.8770 ± 0.0628	0.1608
		HE	0.2677 ± 0.1924	0.2662 ± 0.1147	0.9807
		SE	1.8521 ± 0.5138	2.0569 ± 0.3056	0.2042
	IMF3	FD	1.2873 ± 0.1147	1.3415 ± 0.1302	0.2103
		HE	0.5128 ± 0.1498	0.3943 ± 0.1279	0.0231*
		SE	1.5638 ± 0.4958	1.8837 ± 0.2813	0.0226*
HHb	IMF1	FD	2.0397 ± 0.0592	2.0435 ± 0.0249	0.8235
		HE	0.3315 ± 0.1414	0.2911 ± 0.1060	0.4050
		SE	2.0582 ± 0.3134	2.1100 ± 0.1137	0.5624
	IMF2	FD	1.8475 ± 0.1071	1.8896 ± 0.0764	0.1899
		HE	0.2604 ± 0.1627	0.2232 ± 0.1010	0.4037
		SE	1.9349 ± 0.3615	2.0980 ± 0.0951	0.0925*
	IMF3	FD	1.3343 ± 0.0879	1.3378 ± 0.1063	0.9165
		HE	0.4428 ± 0.1501	0.4822 ± 0.1081	0.4135

		SE	1.7543 ± 0.4024	1.8751 ± 0.3249	0.3959
THI	IMF1	FD	2.0238 ± 0.0791	2.0494 ± 0.0366	0.2660
		HE	0.2837 ± 0.1126	0.2496 ± 0.0958	0.3862
		SE	2.0446 ± 0.3598	2.1181 ± 0.1656	0.4962
	IMF2	FD	1.8565 ± 0.0501	1.8944 ± 0.0418	0.0672*
		HE	0.2683 ± 0.1014	0.3176 ± 0.1233	0.2533
		SE	2.0176 ± 0.3188	2.0767 ± 0.2491	0.5937
	IMF3	FD	1.3841 ± 0.0797	1.4638 ± 0.0813	0.0161*
		HE	0.4245 ± 0.1358	0.3685 ± 0.1281	0.1577
		SE	1.9186 ± 0.2864	2.0471 ± 0.1339	0.1537
TOI	IMF1	FD	2.0301 ± 0.0398	2.0460 ± 0.0237	0.2203
		HE	0.2739 ± 0.1241	0.2337 ± 0.1050	0.3911
		SE	2.1282 ± 0.1294	2.1504 ± 0.1050	0.5408
	IMF2	FD	1.8914 ± 0.0345	1.9067 ± 0.0356	0.2326
		HE	0.2572 ± 0.0896	0.2361 ± 0.0989	0.4779
		SE	2.1117 ± 0.1217	2.1517 ± 0.0739	0.2987
	IMF3	FD	1.4493 ± 0.0927	1.4843 ± 0.0809	0.2176
		HE	0.4377 ± 0.1042	0.3754 ± 0.1113	0.1306
		SE	2.0988 ± 0.1510	2.1091 ± 0.0899	0.8369

Table 2.c – EMD derived features for diabetic subjects who performed adapted physical therapy during exercise.

Adapted Physical Therapy exercise					
Signal	**IMF**	**Features**	**Pre**	**Post**	**p-Value**
O2Hb	IMF1	FD	2.0331 ± 0.0419	2.0348 ± 0.0316	0.8985
		HE	0.2937 ± 0.1059	0.2347 ± 0.0945	0.1194
		SE	2.0183 ± 0.3292	2.0998 ± 0.2322	0.3566
	IMF2	FD	1.8221 ± 0.0800	1.8902 ± 0.0565	0.0114*
		HE	0.2938 ± 0.1408	0.2350 ± 0.1411	0.1411
		SE	1.8882 ± 0.3648	2.0494 ± 0.3045	0.1635
	IMF3	FD	1.3105 ± 0.1077	1.4152 ± 0.0959	0.0083*
		HE	0.5206 ± 0.1550	0.4599 ± 0.1457	0.1754
		SE	1.7135 ± 0.3844	1.9182 ± 0.3068	0.0748*
HHb	IMF1	FD	2.0448 ± 0.0355	2.0446 ± 0.0232	0.9794
		HE	0.2871 ± 0.1089	0.2656 ± 0.0858	0.5404
		SE	2.0586 ± 0.1840	2.1481 ± 0.0822	0.0219*
	IMF2	FD	1.8640 ± 0.0584	1.8983 ± 0.0669	0.1206
		HE	0.2984 ± 0.1084	0.1918 ± 0.1248	0.0063*
		SE	2.0054 ± 0.2017	2.1100 ± 0.0961	0.0350*
	IMF3	FD	1.3466 ± 0.0967	1.4261 ± 0.1220	0.0523*
		HE	0.4484 ± 0.0969	0.4749 ± 0.1192	0.4652

		SE	1.8616 ± 0.3046	2.0061 ± 0.2451	0.1460
THI	IMF1	FD	2.0359 ± 0.0412	2.0426 ± 0.0169	0.5292
		HE	0.2925 ± 0.0981	0.2399 ± 0.0878	0.1075
		SE	1.9827 ± 0.4421	2.1753 ± 0.0333	0.0561*
	IMF2	FD	1.8652 ± 0.0502	1.8937 ± 0.0540	0.1253
		HE	0.2602 ± 0.0959	0.2327 ± 0.1107	0.4541
		SE	1.9110 ± 0.3762	2.1340 ± 0.0628	0.0215*
	IMF3	FD	1.4391 ± 0.1095	1.4508 ± 0.1129	0.6902
		HE	0.3510 ± 0.1760	0.3737 ± 0.1143	0.6117
		SE	1.9658 ± 0.2104	2.0193 ± 0.2694	0.5140
TOI	IMF1	FD	2.0362 ± 0.0400	2.0439 ± 0.0120	0.4352
		HE	0.2891 ± 0.1119	0.2550 ± 0.1005	0.3333
		SE	2.0877 ± 0.3879	2.1758 ± 0.0318	0.3194
	IMF2	FD	1.8806 ± 0.0629	1.8972 ± 0.0212	0.2643
		HE	0.2809 ± 0.0942	0.2333 ± 0.0791	0.0806*
		SE	2.1131 ± 0.1999	2.1430 ± 0.0763	0.5640
	IMF3	FD	1.4291 ± 0.0889	1.4238 ± 0.0738	0.7955
		HE	0.3883 ± 0.1178	0.4686 ± 0.0950	0.0424*
		SE	2.0494 ± 0.1908	2.1075 ± 0.1763	0.3875

Table 3.a – EMD derived features for controls during baseline.

Signal	IMF	Features	Pre	Post	p-Value
			Controls Baseline		
		FD	2.0454 ± 0.0229	2.0464 ± 0.0247	0.9004
	IMF1	HE	0.2053 ± 0.1358	0.2229 ± 0.1152	0.5503
		SE	2.1020 ± 0.1524	2.1176 ± 0.2136	0.8153
		FD	1.9021 ± 0.0487	1.8978 ± 0.0425	0.8221
O2Hb	IMF2	HE	0.2647 ± 0.1679	0.2607 ± 0.1968	0.9582
		SE	2.1862 ± 0.1052	2.1066 ± 0.1988	0.2202
		FD	1.4714 ± 0.1568	1.4264 ± 0.1172	0.3212
	IMF3	HE	0.5015 ± 0.1844	0.5795 ± 0.1632	0.2551
		SE	1.9751 ± 0.3270	2.0306 ± 0.2972	0.6380
		FD	2.0465 ± 0.0271	2.0428 ± 0.0296	0.7238
	IMF1	HE	0.1749 ± 0.1661	0.2164 ± 0.1461	0.5239
		SE	2.0569 ± 0.2376	2.0933 ± 0.2428	0.6864
		FD	1.9126 ± 0.0421	1.8770 ± 0.0717	0.0758*
HHb	IMF2	HE	0.2125 ± 0.1727	0.2552 ± 0.1236	0.4439
		SE	2.0605 ± 0.3111	2.0606 ± 0.2649	0.9988
		FD	1.4051 ± 0.1317	1.4976 ± 0.1628	0.1028
	IMF3	HE	0.6244 ± 0.1776	0.5207 ± 0.1395	0.0747*

		SE	2.0814 ± 0.1737	2.0183 ± 0.3344	0.4821
	IMF1	FD	2.0437 ± 0.0297	2.0369 ± 0.0230	0.3558
		HE	0.2105 ± 0.1309	0.2105 ± 0.1418	0.9990
		SE	2.0551 ± 0.2366	2.1381 ± 0.1581	0.3160
THI	IMF2	FD	1.8856 ± 0.0586	1.8869 ± 0.0401	0.9256
		HE	0.2593 ± 0.1611	0.2685 ± 0.1604	0.8766
		SE	2.1056 ± 0.1526	2.1091 ± 0.2226	0.9582
	IMF3	FD	1.4407 ± 0.1201	1.4475 ± 0.0868	0.8524
		HE	0.5429 ± 0.1116	0.5221 ± 0.1533	0.6399
		SE	2.0991 ± 0.2621	2.0797 ± 0.3413	0.8638
	IMF1	FD	2.0364 ± 0.0277	2.0434 ± 0.0293	0.4471
		HE	0.2012 ± 0.1571	0.2086 ± 0.1215	0.8568
		SE	2.1520 ± 0.0743	2.1934 ± 0.0296	0.0640*
TOI	IMF2	FD	1.9124 ± 0.0565	1.9139 ± 0.0446	0.9380
		HE	0.2547 ± 0.1066	0.2920 ± 0.1431	0.4025
		SE	2.1613 ± 0.1387	2.2011 ± 0.0744	0.1419
	IMF3	FD	1.5229 ± 0.1363	1.4921 ± 0.1328	0.5683
		HE	0.5372 ± 0.1397	0.5019 ± 0.1817	0.5301
		SE	2.1025 ± 0.1443	2.1469 ± 0.1430	0.4273

Table 3.b – EMD derived features for diabetic subjects who performed fit walking during baseline.

Signal	IMF	Features	Pre	Post	p-Value
Fit Walking Baseline					
O2Hb	IMF1	FD	2.0402 ± 0.0143	2.0402 ± 0.0414	0.9972
		HE	0.2749 ± 0.0982	0.2465 ± 0.1008	0.3178
		SE	2.1427 ± 0.1422	2.1475 ± 0.0776	0.9175
	IMF2	FD	1.8881 ± 0.0410	1.9025 ± 0.0541	0.4829
		HE	0.2501 ± 0.1889	0.3321 ± 0.1189	0.1780
		SE	2.0415 ± 0.2602	2.1225 ± 0.1409	0.2974
	IMF3	FD	1.3927 ± 0.1337	1.4599 ± 0.1958	0.2958
		HE	0.4407 ± 0.1692	0.5637 ± 0.1633	0.0379*
		SE	1.7584 ± 0.4826	2.0715 ± 0.2233	0.0467*
HHb	IMF1	FD	2.0469 ± 0.0178	2.0460 ± 0.0265	0.9183
		HE	0.3432 ± 0.1026	0.2165 ± 0.1460	0.0012*
		SE	2.1363 ± 0.1707	2.0821 ± 0.1528	0.4156
	IMF2	FD	1.8821 ± 0.0563	1.9094 ± 0.0422	0.0835
		HE	0.2189 ± 0.1623	0.1481 ± 0.1633	0.2928
		SE	1.9822 ± 0.3059	2.0209 ± 0.2558	0.7317
	IMF3	FD	1.4126 ± 0.0957	1.4837 ± 0.1596	0.1290
		HE	0.3934 ± 0.1557	0.5106 ± 0.2004	0.1405

		SE	1.8099 ± 0.4221	1.9513 ± 0.3532	0.2786
THI	IMF1	FD	2.0470 ± 0.0152	2.0420 ± 0.0321	0.6023
		HE	0.2784 ± 0.0955	0.2320 ± 0.1174	0.1960
		SE	2.1831 ± 0.0289	2.1429 ± 0.0836	0.0870*
	IMF2	FD	1.8855 ± 0.0331	1.8668 ± 0.0662	0.3018
		HE	0.3169 ± 0.1106	0.3153 ± 0.1415	0.9672
		SE	2.1558 ± 0.0693	2.1070 ± 0.1722	0.2871
	IMF3	FD	1.4654 ± 0.0983	1.4294 ± 0.1263	0.3206
		HE	0.3986 ± 0.1276	0.5339 ± 0.1706	0.0045*
		SE	2.0846 ± 0.1394	2.0409 ± 0.2720	0.4677
TOI	IMF1	FD	2.0467 ± 0.0189	2.0488 ± 0.0252	0.8316
		HE	0.2994 ± 0.0768	0.2264 ± 0.0909	0.0353*
		SE	2.1709 ± 0.0371	2.1811 ± 0.0574	0.5963
	IMF2	FD	1.8872 ± 0.0335	1.8922 ± 0.0462	0.7303
		HE	0.2623 ± 0.1462	0.3091 ± 0.1194	0.2806
		SE	2.1665 ± 0.0615	2.2020 ± 0.0561	0.0871*
	IMF3	FD	1.4802 ± 0.0925	1.4952 ± 0.1291	0.7048
		HE	0.4149 ± 0.1192	0.4980 ± 0.0946	0.0538*
		SE	2.1358 ± 0.1363	2.1786 ± 0.0615	0.2538

Table 3.c – EMD derived features for diabetic subjects who performed adapted physical therapy during baseline.

Signal	IMF	Features	Pre	Post	p-Value
			Adapted Physical Therapy baseline		
Signal	**IMF**	**Features**	**Pre**	**Post**	**p-Value**
O2Hb	IMF1	FD	2.0464 ± 0.0204	2.0411 ± 0.0222	0.5074
		HE	0.2550 ± 0.0706	0.1646 ± 0.1516	0.0221*
		SE	2.1201 ± 0.0928	2.1304 ± 0.1386	0.8058
	IMF2	FD	1.8770 ± 0.0629	1.8998 ± 0.0576	0.1990
		HE	0.2986 ± 0.1532	0.2517 ± 0.1394	0.3590
		SE	1.9940 ± 0.2991	2.0929 ± 0.1933	0.1782
	IMF3	FD	1.4647 ± 0.0960	1.4648 ± 0.1103	0.9969
		HE	0.4475 ± 0.1913	0.5148 ± 0.1401	0.2178
		SE	1.8484 ± 0.4088	2.0090 ± 0.3052	0.2542
HHb	IMF1	FD	2.0413 ± 0.0212	2.0341 ± 0.0267	0.4408
		HE	0.2644 ± 0.0944	0.1750 ± 0.1105	0.0106*
		SE	2.1131 ± 0.1409	2.0813 ± 0.1570	0.5405
	IMF2	FD	1.8965 ± 0.0478	1.8930 ± 0.0563	0.8295
		HE	0.2571 ± 0.1085	0.2553 ± 0.1962	0.9680
		SE	2.0413 ± 0.2771	2.0906 ± 0.2070	0.4647
	IMF3	FD	1.4641 ± 0.1005	1.4617 ± 0.1320	0.9416
		HE	0.4313 ± 0.1202	0.5413 ± 0.2080	0.0404*

		SE	2.0441 ± 0.2864	2.0478 ± 0.2077	0.9626
THI	IMF1	FD	2.0332 ± 0.0438	2.0453 ± 0.0198	0.2621
		HE	0.2578 ± 0.1074	0.2025 ± 0.1021	0.0913*
		SE	2.0542 ± 0.3087	2.1634 ± 0.1212	0.1571
	IMF2	FD	1.8700 ± 0.0670	1.8815 ± 0.0388	0.4296
		HE	0.2502 ± 0.1427	0.2928 ± 0.1360	0.2516
		SE	2.0493 ± 0.1925	2.1349 ± 0.1254	0.1343
	IMF3	FD	1.4634 ± 0.0924	1.4507 ± 0.1098	0.6559
		HE	0.4860 ± 0.1690	0.5453 ± 0.1681	0.3544
		SE	2.0658 ± 0.1703	2.0473 ± 0.2638	0.7678
TOI	IMF1	FD	2.0391 ± 0.0436	2.0520 ± 0.0281	0.3381
		HE	0.2579 ± 0.0983	0.2152 ± 0.1278	0.2968
		SE	2.0916 ± 0.3955	2.1754 ± 0.0557	0.3644
	IMF2	FD	1.8877 ± 0.0906	1.9020 ± 0.0395	0.4954
		HE	0.2476 ± 0.1237	0.3041 ± 0.1037	0.1195
		SE	2.1799 ± 0.0721	2.1904 ± 0.0622	0.6609
	IMF3	FD	1.4686 ± 0.0860	1.4524 ± 0.0902	0.5839
		HE	0.4603 ± 0.1281	0.5437 ± 0.1576	0.0586*
		SE	2.0963 ± 0.1273	2.1751 ± 0.1061	0.0240*

Table 4.

Five most discriminant variables among groups in the different conditions, as obtained by MANOVA. Each variable is uniquely indicated by a signal (O2Hb, HHb, or TOI), number of the IMF, and feature.

(FD –Fractal Dimension; HE – Hurst Exponent; SE – Sample Entropy)

| Before training (baseline)	After training (baseline)	Before training (exercise)	After training (exercise)
HHb IMF1 FD	HHb IMF1 FD	HHb IMF1 FD	HHb IMF1 FD
HHb IMF1 HE	HHb IMF2 FD	HHb IMF1 HE	HHb IMF1 HE
TOI IMF2 SE	TOI IMF2 FD	HHb IMF1 SE	HHb IMF1 SE
TOI IMF3 SE	TOI IMF3 SE	HHb IMF2 FD	HHb IMF2 HE
TOI IMF3 HE	TOI IMF3 HE	O2Hb IMF2 FD	TOI IMF3 HE

FIGURES

Figure 1

O2Hb signal (red line) and HHb (blue line) of a subject performing the exercise. During the contraction the local concentration of O2Hb decreases whereas that of HHb increases.
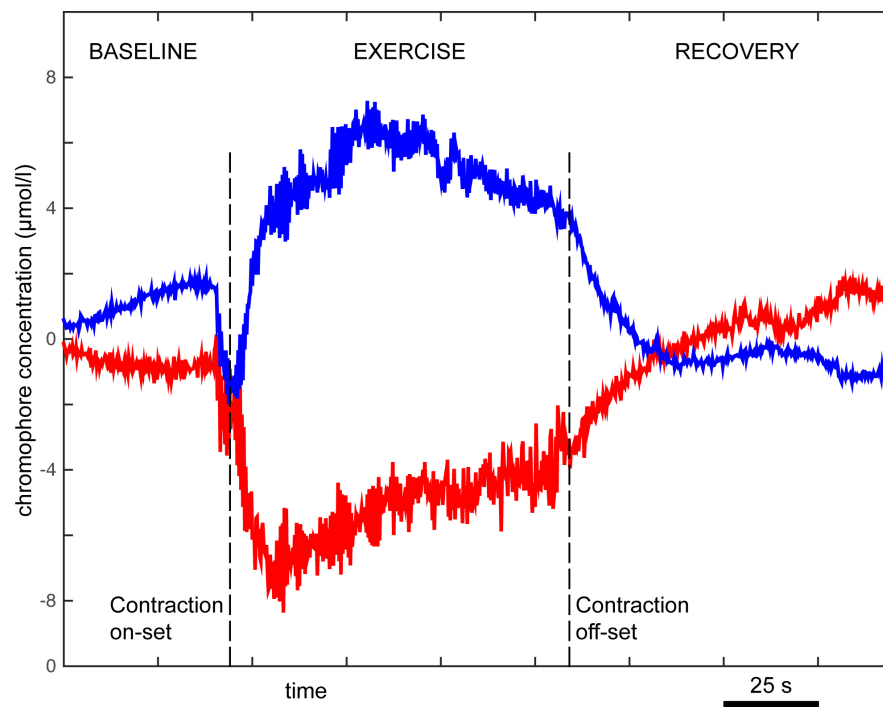
Figure 2

MANOVA analysis during baseline: (left panel) before physical training; (right panel) after physical training. Black diamonds indicate healthy controls, white circles the diabetic subjects who performed fit walking, and the gray squares the diabetic subjects who performed the adapted physical therapy. The groups distance is reduced after training and the dimension of the sample decreased from 2 to 1.
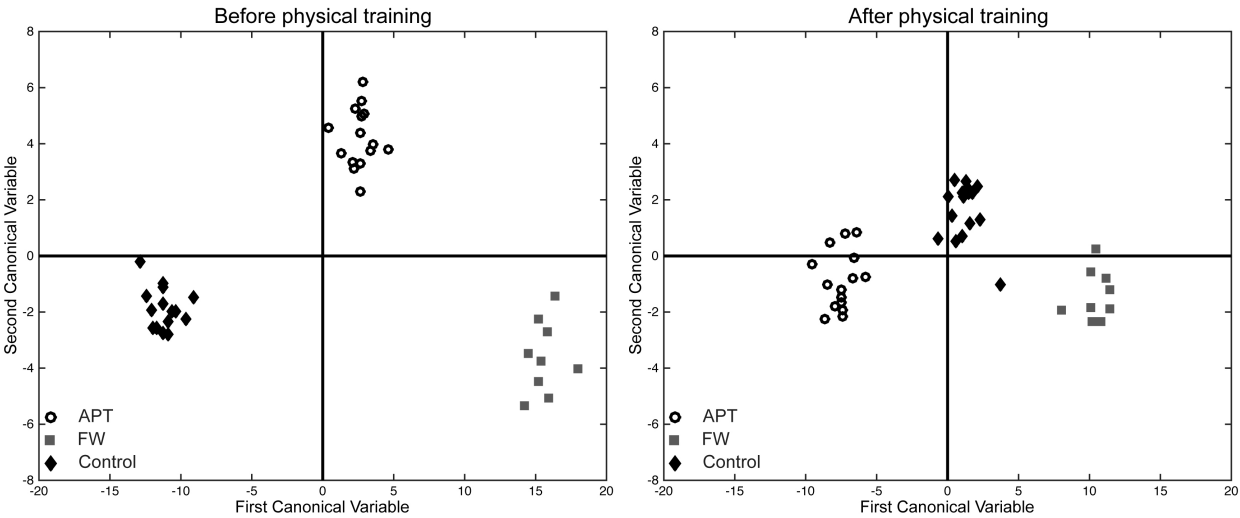
Figure 3

MANOVA analysis during exercise: (left panel) before physical training; (right panel) after physical training. Black diamonds indicate healthy controls, white circles the diabetic subjects who performed fit walking, and the gray squares the diabetic subjects who performed the adapted physical therapy. The groups distance is reduced after training and the dimension of the sample decreased from 1 to 0.